

Fast Low-Angle B1 Mapping

Caroline Le Ster^{1,2}, Giulio Gambarota¹, Eric Brillet³, Olivier Beuf⁴, and Hervé Saint-Jalmes^{1,5}

¹INSERM UMR 1099, Université de Rennes 1, Rennes, France, ²Siemens Healthcare, Saint-Denis, France, ³Department of Imaging, Rennes University Hospital, Rennes, France, ⁴Université de Lyon, CREATIS, CNRS UMR 5220, INSERM U1044, INSA-Lyon, Université Lyon 1, Villeurbanne, France, ⁵Centre Eugène Marquis, CRLCC, Rennes, France

Target audience

MR physicists interested in mapping the B1 field at low flip angles with no dedicated sequence requirement.

Purpose

Quantitative MR methods often require the knowledge of the local B1 field. Many B1 mapping methods have been developed, but few of them are suited to measure low flip angles. Here we use the Low Angle Method¹ coupled with EPI (LAM EPI) to acquire multislice B1 maps on a phantom and in vivo on the brain and the abdomen (breathold acquisition). We compare our results to the reference B1 mapping Double Angle Method² (DAM) and the classical LAM method (LAM FLASH).

Methods

In the LAM method, two gradient echo images are acquired with long TRs to suppress their T1 dependence: S_α with the prescribed flip angle α and S_{90} with the prescribed flip angle 90° . The actually applied flip angle is: $\alpha = \arcsin(S_\alpha/S_{90})$. Because the signal is proportional to a sine it varies slowly around 90° , it is then relatively insensitive to small variations of B1 around 90° .

In this study we acquire the two images with an echo-planar imaging (EPI) readout: S_α is acquired with a long TR (TR_α) so that the longitudinal magnetization Mz has fully recovered before the acquisition of the second image S_{90} . Moreover, the TR of the 90° acquisition (TR_{90}) is set relatively short to last just the time to acquire the signal (figure 1) and allow short breathhold acquisitions. The minimal TR_α for a full recovery of Mz following a pulse α is: $TR/T1 = \log[(1 - \cos\alpha + \epsilon \cos\alpha)/\epsilon]$ (figure 2).

We mapped the B1 field at 5° , 10° and 20° on a phantom ($T1=1000\text{ms}$, agar at 2% and gadolinium at 0.2%) and on healthy volunteers ($T1_{\text{max}}=4000\text{ms}$, brain and abdomen) on a 1.5T Siemens Aera scanner.

Phantom imaging: EPI images acquisition parameters: flip angle= 5° , 10° , 20° , $TR_\alpha=15000\text{ms}$, $TR_{90}=15000\text{ms}$, TE=32ms, slice thickness=10mm, 10 slices, matrix size=98x98, acquisition time (TA) 2x0:15. FLASH images: flip angle/ $TR_\alpha=5^\circ/1000\text{ms}$, $10^\circ/1000\text{ms}$, $20^\circ/2000\text{ms}$, $40^\circ/2000\text{ms}$ and $TR_{90}=5000\text{ms}$, TE=4.4ms, acceleration factor 2, slice thickness=10mm, 3 slices, matrix size=128x128, TA 2:20+6:00. EPI images were used to map the B1 field with LAM (LAM EPI) and FLASH images were used to map the B1 field with both LAM (LAM FLASH) and DAM.

In vivo imaging: EPI parameters: flip angle/ $TR_\alpha=5^\circ/2000\text{ms}$, $10^\circ/4000\text{ms}$, $20^\circ/8000\text{ms}$ and $TR_{90}=2000\text{ms}$, TE=32ms, slice thickness of 10mm, 18 slices, matrix size of 98x98, fat suppression, TA 0:17.

Analysis: The precision of these methods was analysed by error propagation and Monte Carlo simulations. For Monte Carlo simulations, we simulated 3000 samples of the signal with an added Gaussian noise. The performances of LAM and DAM were simulated using an SNR of 100.

Results

B1 maps are more accurate with LAM than DAM for flip angles lower than 45° (figure 3). These results are confirmed on the phantom (figure 4): the DAM is unable to compute B1 maps for low flip angles. DAM is more robust to error propagation for high flip angles but LAM remains efficient until 70° . Acquisitions with EPI and FLASH give similar flip angles, as seen on the slice profiles of figure 4. The B1 maps are smooth in the brain and they suffer from some artefacts in the abdomen due to the movement of the organs and imperfect breathhold (figure 5). However these artefacts are limited here by the acquisition of the two EPI images during the same apnea, which results in two superimposable images. The algorithm is not able to compute flip angles in areas with movement and in tissues with short T2* because of the low signals caused by the long TE.

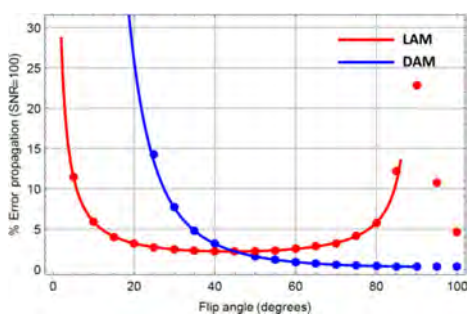


Fig 3: Relative error on the measured flip angle derived from analytical expressions (lines) and Monte Carlo simulations (points).

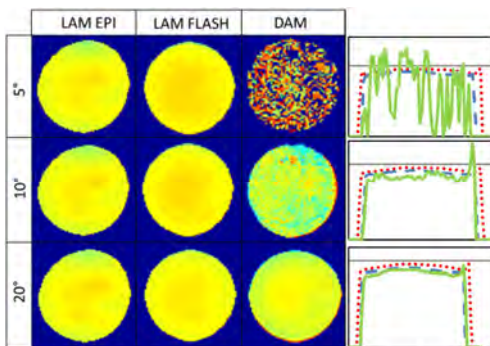


Fig 4: Phantom B1 maps and slice profiles for LAM EPI (points), LAM FLASH (dots) and DAM (line).

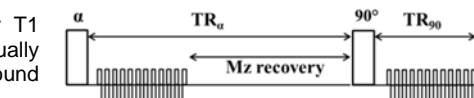


Fig 1: Diagram of the LAM EPI sequence

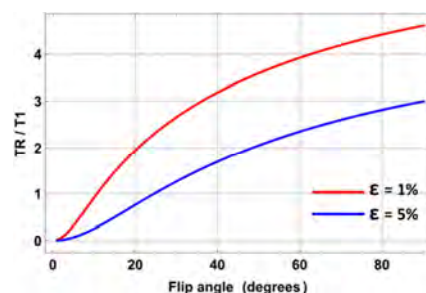


Fig 2: Minimal $TR/T1$ for a full recovery of Mz as a function of the prescribed flip angle. For $T1=1000\text{ms}$ at 20° , the signal is independent of T1 for $TR>2000\text{ms}$.

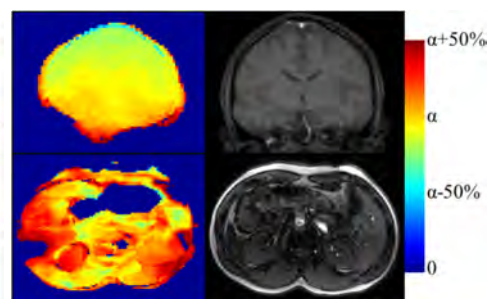


Fig 5: B1 maps of the head (5°) and the abdomen (20°) measured with LAM EPI.

Discussion / Conclusion

These results confirm that LAM is particularly suited to measure low flip angles, whereas DAM is efficient for high flip angles. The LAM EPI method allows multislice B1 mapping in a clinically acceptable time (breathhold) without any dedicated sequence requirement. EPI images however suffer from distortions artefacts and their long TE might suppress tissues with short T2*.

References

1. Balezeau F, et al. Mapping of low flip angles in magnetic resonance. Physics in medicine and biology 56.20 (2011): 6635.
2. Insko, E. K., and L. Bolinger. Mapping of the radiofrequency field. Journal of Magnetic Resonance, Series A 103.1 (1993): 82-85.